
Topology-Preserving Data Augmentation for Ring-Type Polygon Annotations

Sudip Laudari^{*1} Sang Hun Baek¹

Abstract

Geometric data augmentation is widely used in segmentation pipelines and typically assumes that polygon annotations represent simply connected regions. However, in structured domains such as architectural floorplan analysis, ring-type regions are often encoded as a single cyclic polygon chain connecting outer and inner boundaries. During augmentation, clipping operations may remove intermediate vertices and disrupt this cyclic connectivity, breaking the structural relationship between the boundaries. In this work, we introduce an order-preserving polygon augmentation strategy that performs transformations in mask space and then projects surviving vertices back into index-space to restore adjacency relations. This repair maintains the original traversal order of the polygon and preserves topological consistency with minimal computational overhead. Experiments demonstrate that the approach reliably restores connectivity, achieving near-perfect Cyclic Adjacency Preservation (CAP) across both single and compound augmentations.

Keywords: Data Augmentation, Polygon Segmentation, Topology Preservation, Floorplan Analysis

1. Introduction

Segmentation tasks are widely used to extract object boundaries and spatial structures from images (Long et al., 2015; Ronneberger et al., 2015). In many datasets, object regions are represented using closed polygon boundaries that describe the geometry of the target area. However, real-world environments often contain regions with more complex structures, such as corridors, courtyards, walls and spaces with interior voids. These configurations frequently appear in architectural floorplans and other structured vision domains (Liu et al., 2018; Dodge et al., 2017; Mnih,

2013). Accurate polygon representations are therefore essential for tasks such as raster-to-vector conversion, layout analysis, spatial measurement, and geometric reconstruction (Lin et al., 2014; Liu et al., 2018; Acuna et al., 2018; Dodge et al., 2017; Girard et al., 2021).

To improve the robustness and generalization of segmentation models in such tasks, data augmentation is commonly applied during preprocessing (Shorten & Khoshgoftaar, 2019). Transformations such as rotation, scaling, cropping, and flipping increase data diversity and help reduce overfitting (Perez & Wang, 2017). Modern augmentation frameworks, including Albumentations (Buslaev et al., 2020) and imgaug (Jung, 2018), support polygon-based annotations and jointly transform images and their vertex coordinates. As a result, these tools have become standard components of many segmentation pipelines.

However, most augmentation pipelines implicitly assume that each polygon represents a simply connected region. In architectural datasets, regions with interior voids are often encoded as a single cyclic polygonal chain (see Figure 1), where implicit bridge and closure edges connect the outer and inner boundary segments. While affine transformations preserve cyclic ordering in theory, practical augmentation operations may remove vertices when polygons are cropped or extend beyond image boundaries. Consequently, the cyclic structure of the polygon can be disrupted, breaking the intended ring representation.

This failure mode is often difficult to detect. At the pixel level, the augmented region may still appear visually correct, while at the annotation level the polygon may no longer preserve its intended topology. This can cause a single semantic region to become represented as multiple disconnected fragments, introducing inconsistencies in training data, visualization, and downstream geometric reasoning (Mikolajczyk et al., 2005; Benenson et al., 2019; Cordts et al., 2016). In practice, we observe this phenomenon frequently in datasets containing ring-type regions.

To address this issue, we introduce an order-preserving connectivity repair strategy for polygon-based annotation datasets. The approach combines mask-based geometric augmentation with vertex index projection and cyclic repair to restore adjacency relations after vertex deletion. The resulting procedure is lightweight, integrates easily into

¹Independent Researcher. Correspondence to: Sudip Laudari <sudiplaudari@gmail.com>, Sang Hun Baek <shawnbbaek@gmail.com>.

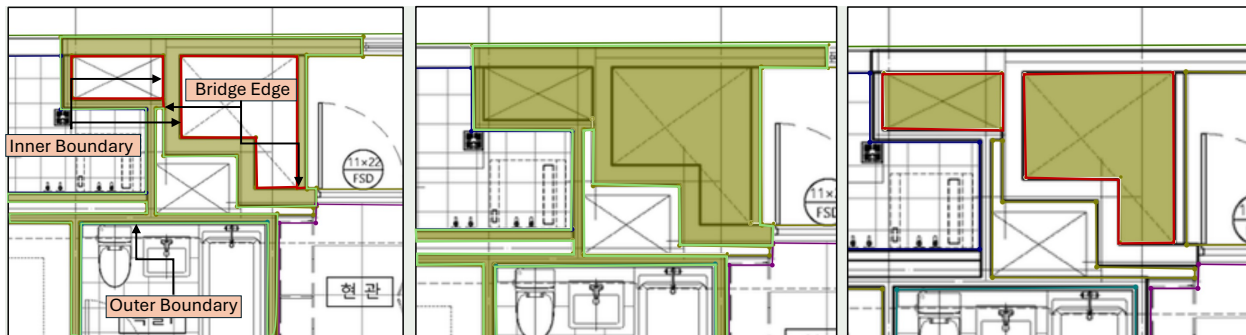


Figure 1. Failure of ring-type polygon annotations under geometric augmentation. **Left:** Ground-truth polygon with a narrow bridge connector and inner boundaries are shown in red color and outer boundary in green color. Each corner has a vertex(keypoints), and mask (olive color) shows ring type annotation generated because of wall design. **Middle and Right:** Representative failure cases after augmentation, where the connector is disrupted and the polygon topology is no longer preserved, yielding separate outer mask from outer boundary and inner boundary masks from inner boundary mask.

existing augmentation pipelines, and preserves topology-consistent polygon annotations under geometric transformations.

2. Related Work

Data augmentation is a fundamental component of modern segmentation pipelines, improving robustness, generalization, and invariance to geometric transformations (Shorten & Khoshgoftaar, 2019; Perez & Wang, 2017). Common operations such as rotation, scaling, translation, cropping, and flipping are widely applied across visual recognition tasks (Krizhevsky et al., 2012). In practice, augmentation libraries such as Albumentations (Buslaev et al., 2020), imgaug (Jung, 2018), Augmentor (Bloice et al., 2017), and the recently proposed polygon augmentation library AugmenTory (Ghahremani et al., 2024) provide efficient mechanisms for jointly transforming images and their corresponding polygon annotations. These frameworks are typically used with COCO-style polygon encodings (Lin et al., 2014), where object regions are represented as ordered vertex sequences. Such polygon annotations are widely adopted in large-scale datasets such as COCO (Lin et al., 2014) and are commonly generated using annotation tools such as LabelMe (Russell et al., 2008). They are particularly important in structured vision domains including architectural layouts, floorplans, maps, and technical drawings (Dodge et al., 2017; Kaleva & Kämäräinen, 2019; Zheng et al., 2020), where polygon annotations capture structural relationships between boundaries and spatial regions. While existing augmentation frameworks correctly transform vertex coordinates under geometric operations, they primarily focus on spatial consistency and typically assume that polygon connectivity remains valid after augmentation.

In practical machine learning pipelines, augmentation is commonly integrated into training frameworks and dataset

platforms (Shorten & Khoshgoftaar, 2019; Krizhevsky et al., 2012; Chen et al., 2021; 2022; Zoph et al., 2020). For example, modern detection and segmentation frameworks such as YOLO (Bochkovskiy et al., 2020; Myshkovskiy et al., 2025) incorporate online augmentation during training, where images and their annotations are transformed on-the-fly to improve robustness. Likewise, recent work on polygon-based augmentation such as AugmenTory (Ghahremani et al., 2024) highlights that polygon and mask annotations are routinely augmented using geometric transformations in YOLO-style instance segmentation models. These systems rely heavily on geometric transformations applied directly to vertex coordinates or derived contours. However, when polygons are clipped by image boundaries or crop operations, vertices may be removed, potentially disrupting the original adjacency relationships encoded in the polygon sequence.

To mitigate such issues, some approaches perform augmentation in mask space rather than directly manipulating polygon vertices. In these methods, polygons are first rasterized into binary masks, geometric transformations are applied to the masks, and the resulting contours or polygonal boundaries are extracted afterward (Shorten & Khoshgoftaar, 2019; Liang et al., 2020; Lazarow et al., 2022; Ghahremani et al., 2024). While this strategy simplifies augmentation pipelines, the contour re-extraction process is inherently resolution dependent. As a result, narrow connections such as the bridge between outer and inner boundaries in ring-shaped regions may collapse during rasterization, merging interior holes with the background or fragmenting the region into multiple components. More generally, theoretical frameworks such as topological data analysis and persistent homology study connectivity and shape invariants under continuous transformations (Carlsson, 2009; Edelsbrunner et al., 2008), and recent work has introduced topology-aware loss functions to encourage connectivity

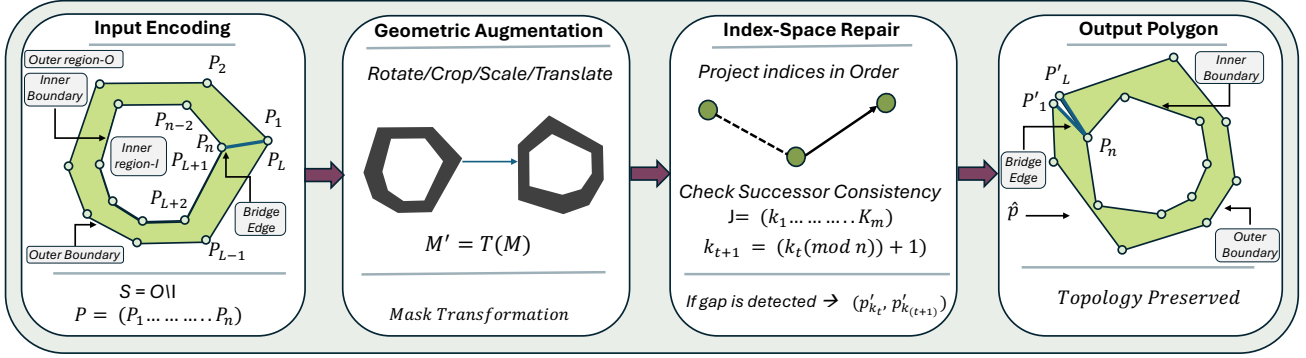


Figure 2. Overview of the proposed topology-preserving augmentation pipeline for ring-type polygons. From left to right: the input ring region is encoded as a single cyclic polygon chain $P = (p_1, \dots, p_n)$ representing outer and inner boundaries. The polygon is rasterized and geometric augmentation is applied in mask space, $M' = T(M)$ (e.g., rotate, crop, scale, translate). The surviving polygon indices are then projected in order and successor consistency is checked. If the order is preserved, the polygon remains valid; otherwise, gaps in the index sequence are repaired using the proposed index-space reconnection method. The resulting polygon \hat{P} forms a single closed cyclic chain with preserved ring topology.

preservation during model training (Hu et al., 2019). However, these methods operate on pixel-level predictions and do not address structural corruption that can arise earlier in the pipeline when polygon annotations themselves are altered during augmentation.

Despite the widespread use of polygon-based augmentation, the specific problem of cyclic connectivity failure in single-chain ring encodings has received little attention. Existing augmentation frameworks ensure that vertex coordinates are transformed consistently but do not explicitly enforce the adjacency relationships required to maintain ring semantics. In contrast, our work introduces a lightweight repair mechanism that restores cyclic connectivity after augmentation while remaining compatible with existing polygon-based workflows.

3. Method

Let $P = (p_1, p_2, \dots, p_n)$ denote a polygon annotation encoded as a cyclic vertex sequence. In practical datasets, polygon annotations may represent both simply connected regions and ring-type regions containing interior voids. Examples include architectural structures such as walls, corridors, and exterior spaces surrounding floor boundaries, where the geometry is defined by an ordered sequence of vertices.

To ensure reliable data augmentation preprocessing for computer vision pipelines, we introduce an augmentation procedure consisting of four stages: (1) rasterizing the polygon into a binary mask, (2) applying geometric augmentation in mask space, (3) projecting surviving vertices back into index space, and (4) restoring cyclic connectivity among the remaining vertices.

This procedure preserves the original traversal order of the

polygon while ensuring that the augmented annotation remains topologically consistent.

3.1. Ring-Type Polygon Encoding

We represent a ring-type region as

$$S = O \setminus I,$$

where $O \subset \mathbb{R}^2$ denotes the outer region boundary and $I \subset O$ denotes an interior hole within the region.

In many annotation formats such as COCO, regions containing holes are typically represented using multiple independent polygons. In contrast, architectural datasets often encode ring-type regions as a single cyclic polygon chain when floorplan structures are traced or reconstructed. In this representation, both the outer boundary and the inner boundary are stored within a single ordered sequence of vertices.

We therefore represent the polygon as an ordered vertex sequence

$$P = (p_1, p_2, \dots, p_n),$$

where each vertex $p_i \in \mathbb{R}^2$ corresponds to a point in the image coordinate system.

The sequence is partitioned into two segments:

- **Outer boundary:** $\mathcal{B}_{out} = (p_1, \dots, p_L)$
- **Inner boundary:** $\mathcal{B}_{in} = (p_{L+1}, \dots, p_n)$

These segments are connected through two edges that maintain the cyclic traversal of the polygon (see Figure 2):

$$e_b = (p_L, p_{L+1})$$

where e_b denotes the bridge edge connecting the outer and inner boundaries.

$$e_c = (p_n, p_1)$$

where e_c denotes the closure edge completing the cyclic polygon.

This encoding allows a single cyclic vertex chain to represent regions containing interior holes while remaining compatible with standard polygon annotation formats.

3.2. Mask-Based Geometric Augmentation

Direct augmentation of polygon vertices may break connectivity when vertices fall outside image boundaries. To avoid this issue, we perform geometric transformations in mask space.

The polygon P is first rasterized into a binary mask M . Geometric augmentation is then applied as

$$M' = T(M)$$

where T denotes an affine transformation such as rotation, scaling, translation, or cropping.

Each polygon vertex p_i is associated with an index that preserves the original traversal order of the polygon. After augmentation, the boundary of the transformed mask M' is extracted and used as a geometric reference for vertex projection. For each original vertex index, we search for the nearest boundary point on M' that corresponds to the transformed location of the vertex.

If the transformed vertex lies outside the image or outside the valid mask region due to cropping or clipping, the original vertex is discarded. In such cases, the clipping boundary may introduce new intersection points that become additional vertices on the augmented polygon.

The surviving vertices are then projected back into index space to reconstruct the polygon representation while preserving the original cyclic ordering (see Figure 3).

3.3. Order-Preserving Connectivity Repair

Let $J = (k_1, k_2, \dots, k_m) \subset \{1, \dots, n\}$ denote the indices of vertices that remain valid after augmentation, ordered according to their original cyclic order, where $m \leq n$.

To restore cyclic connectivity, we enforce successor consistency among surviving indices. For each pair of consecutive indices (k_t, k_{t+1}) with $k_{m+1} := k_1$, we check whether the original successor relation holds:

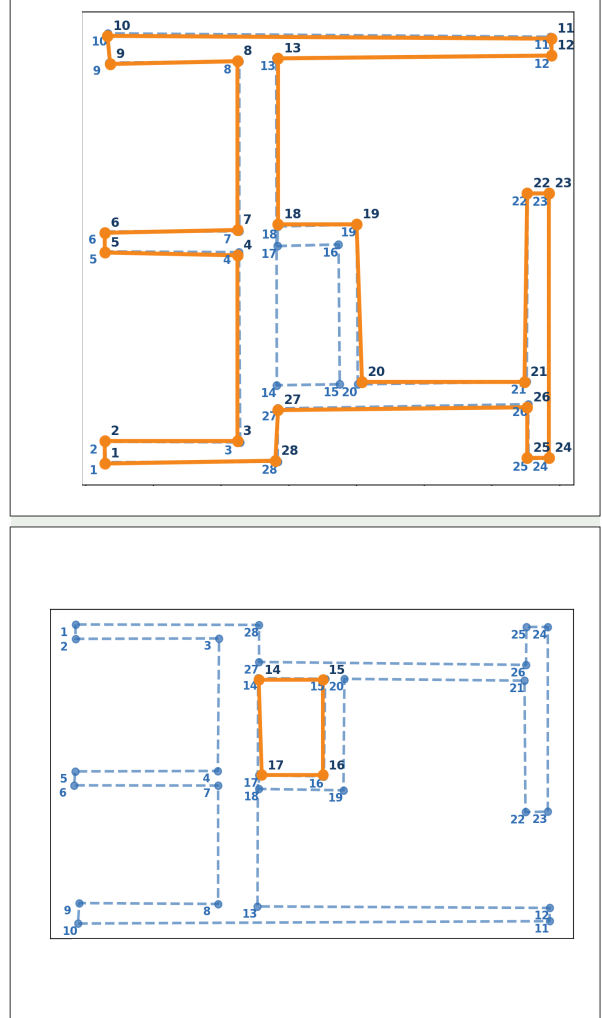


Figure 3. Vertex projection after mask-based augmentation. The dashed blue polygon shows the original vertex sequence with indices, while the solid orange polygon shows the augmented polygon. Surviving vertices are projected onto the augmented boundary and retain their original indices, preserving the cyclic ordering of the polygon chain. Vertices removed by clipping are discarded, allowing the augmented polygon to be reconstructed while maintaining index consistency.

$$k_{t+1} = (k_t \pmod{n}) + 1$$

If this condition is violated, a gap in the original index sequence indicates that intermediate vertices were removed during augmentation. We then reconnect the surviving vertices by enforcing the directed edge

$$(p'_{k_t}, p'_{k_{t+1}})$$

in the repaired polygon \hat{P} .

This process preserves the original traversal direction while

restoring adjacency relations across surviving vertices.

Algorithm 1 Order-Preserving Polygon Augmentation and Connectivity Repair

- 1: **Input:** Original polygon $P = (p_1, p_2, \dots, p_n)$, augmentation transform T
- 2: **Output:** Repaired cyclic polygon chain \hat{P}
- 3: Rasterize P into binary mask M
- 4: Apply geometric augmentation: $M' \leftarrow T(M)$
- 5: Project original vertices onto M' and extract surviving index set $J = (k_1, k_2, \dots, k_m)$
- 6: Sort J according to original cyclic order
- 7: Initialize $\hat{P} \leftarrow \emptyset$
- 8: **for** $t = 1$ to m **do**
- 9: $i \leftarrow k_t$
- 10: $j \leftarrow k_{((t \bmod m)+1)}$
- 11: Add directed edge (p'_i, p'_j) to \hat{P}
- 12: **end for**
- 13: **return** \hat{P}

3.4. Topological Consistency

Because ring topology is defined by cyclic successor relations in the vertex sequence, maintaining adjacency among surviving indices preserves the structural transitions between \mathcal{B}_{out} and \mathcal{B}_{in} . The resulting polygon \hat{P} therefore forms a single closed cyclic chain that remains consistent with the original ring encoding.

3.5. Implementation and Complexity

The repair procedure operates in $O(m)$ time, where m is the number of surviving vertices after augmentation ($m \leq n$). All operations are performed in index space and therefore introduce negligible computational overhead compared with standard geometric augmentation operations. Because the method avoids contour reconstruction or polygon re-detection, it remains lightweight and can be easily integrated into existing augmentation pipelines.

4. Experimental Setup

Our evaluation focuses on the structural correctness of polygon annotations under geometric data augmentation. In particular, we analyze whether augmentation pipelines preserve the cyclic topology of ring-type polygons and whether the proposed repair strategy restores structural consistency when vertex deletion occurs.

Unlike conventional segmentation studies, our experiments evaluate annotation-level topology rather than downstream segmentation accuracy. This allows us to directly measure how augmentation procedures affect the structural integrity of polygon representations.

All augmentation methods are applied using identical parameter ranges. Metrics are computed per semantic class and averaged across samples.

4.1. Augmentation Setup

Augmentation Parameters: We evaluate commonly used geometric augmentations in segmentation pipelines, including rotation, scaling, translation, cropping, and horizontal flipping. The parameter ranges follow standard augmentation practices and are summarized in Table 1. Color-based augmentations are excluded since they do not alter polygon geometry.

Table 1. Geometric augmentation parameters evaluated in this study.

Augmentation	Parameter	Range
Rotation	Angle	$[-30^\circ, 30^\circ]$
Scaling (in/out)	Scale factor	$[0.7, 1.3]$
Cropping	Crop scale	$[0.6, 1.0]$
Rotation + Cropping	Angle / scale	$[-30^\circ, 30^\circ], [0.6, 1.0]$
Translation	Shift ratio	$[-0.1, 0.1]$ (x, y)
Flipping	H / V flip	Probability = 0.5

Baselines: We compare our proposed method against widely used augmentation workflows to assess cyclic topology preservation under practical conditions.

- **YOLOv11 Pipeline (Ultralytics, 2024).** Represents a typical training-time augmentation strategy used in modern detection and segmentation frameworks. Geometric transformations are applied during model training, and polygon annotations are transformed jointly with images. However, no explicit validation of cyclic vertex adjacency is performed after vertex removal.
- **Roboflow Augmentation (Roboflow, Inc., 2023).** Represents a preprocessing-based augmentation workflow widely used in dataset preparation platforms. Polygon vertices are transformed according to geometric mappings, but cyclic index adjacency is not enforced when vertices are removed due to clipping or cropping.
- **Ours (Proposed).** Uses the Albumentations geometric engine (Buslaev et al., 2020) for spatial transformations and applies our index-preserving repair module to restore cyclic adjacency among surviving vertices.

4.2. Evaluation Metric: Cyclic Adjacency Preservation (CAP)

To quantify structural integrity of polygon annotations, we introduce the *Cyclic Adjacency Preservation (CAP)* metric.

Let the original polygon be defined by the cyclic index set $I = \{1, \dots, n\}$ with successor function

$$\text{succ}(i) = (i \bmod n) + 1.$$

After augmentation and boundary clipping, let

$$J = (k_1, k_2, \dots, k_m)$$

denote the ordered set of surviving vertex indices, where $m \leq n$ and $k_{m+1} := k_1$.

CAP measures the proportion of surviving adjacency relations that remain consistent with the original cyclic order:

$$\text{CAP}(P \rightarrow P') = \frac{1}{m} \sum_{t=1}^m \mathbb{I}[k_{t+1} = \text{succ}(k_t)], \quad (1)$$

where $\mathbb{I}[\cdot]$ denotes the indicator function.

The metric $\text{CAP} \in [0, 1]$ equals 1.0 only when all surviving vertices maintain their original cyclic successor relations. Unlike geometric overlap metrics such as mIoU, CAP evaluates preservation of the polygon’s connectivity structure rather than spatial overlap.

Importantly, CAP does not penalize legitimate vertex removal caused by cropping. Instead, it detects discontinuities in the remaining vertex sequence that break cyclic connectivity.

For a dataset containing N ring-type polygon instances, we report the mean Cyclic Adjacency Preservation:

$$\overline{\text{CAP}} = \frac{1}{N} \sum_{i=1}^N \text{CAP}(P_i \rightarrow P'_i). \quad (2)$$

5. Results

The quantitative evaluation of cyclic topology preservation under rotation augmentation is summarized in Table 2. Standard augmentation pipelines frequently introduce cyclic adjacency violations because vertices may be removed during clipping or cropping operations. When intermediate vertices disappear, the successor relationships encoded in the original polygon sequence are disrupted, producing fragmented polygon chains and inconsistent topology.

The proposed repair mechanism addresses this issue by restoring adjacency relations among surviving vertices through successor consistency in index space. As reflected in Table 2, the proposed method achieves CAP values close to 1.0, indicating near-perfect preservation of the original cyclic polygon structure after augmentation. In contrast, baseline pipelines exhibit substantially lower CAP values, suggesting that conventional augmentation strategies do not

reliably maintain the structural integrity of ring-type polygons. These failures occur because geometric operations such as cropping or boundary clipping remove intermediate vertices without updating the cyclic adjacency relations encoded in the polygon sequence. In addition, some augmentation pipelines reconstruct polygons from rasterized masks, which can alter vertex ordering or introduce dense contour points that further disrupt the original cyclic structure.

Table 2. Mean Cyclic Adjacency Preservation (CAP) under rotation augmentation. Higher values indicate better preservation of cyclic polygon topology.

Method	CAP (\uparrow)
YOLO Augmentation	0.3278
Roboflow	0.5497
Ours	0.9758

Table 3. Mean Cyclic Adjacency Preservation (CAP) across geometric augmentations using the proposed repair strategy.

Augmentation	CAP (\uparrow)
Rotation	0.9774
Cropping	0.9840
Scaling	0.9827
Flip	0.9869
Rotation + Cropping	0.9748

Qualitative comparisons across augmentation pipelines further illustrate these differences (Figures 4–6). Under Roboflow augmentation, clipping during geometric transformations removes the bridge connector between the outer and inner boundaries (Figure 4). As a result, the polygon chain becomes fragmented and the annotation splits into separate masks representing the outer and inner regions, breaking the intended ring topology.

A different behavior is observed in the YOLO training augmentation pipeline (Figure 5). Although the topology collapse seen in Roboflow does not occur, the augmentation introduces an excessive number of boundary vertices along the outer contour. This produces an inflated polygon representation with more keypoints than required, altering the original boundary structure. Such behavior likely arises from raster-to-vector contour extraction commonly used in augmentation frameworks. Instead of directly transforming the original vertex indices, the augmented mask is converted back into a polygon by re-extracting contours, resulting in a dense sequence of pixel-aligned vertices that deviates from the sparse and structurally consistent representation of the ground truth.

In contrast, the proposed repair strategy preserves the cyclic ordering of vertices and reconstructs the polygon chain after augmentation by restoring missing successor relations



Figure 4. Qualitative results using Roboflow augmentation. The left panel shows the ground truth polygon with a ring structure. The middle and right panels illustrate failure cases after augmentation, where clipping and rotation remove the bridge connection between the outer and inner boundaries. As a result, the original ring polygon becomes fragmented and is incorrectly represented as two independent polygons corresponding to the outer and inner regions.



Figure 5. Examples illustrating topology failure under YOLO training augmentation with default parameters. The upper row shows the ground truth ring-type polygon annotations, while the lower row shows the augmented outputs. After augmentation, the interior hole is lost and the region is incorrectly represented as a single large polygon, breaking the intended ring topology.

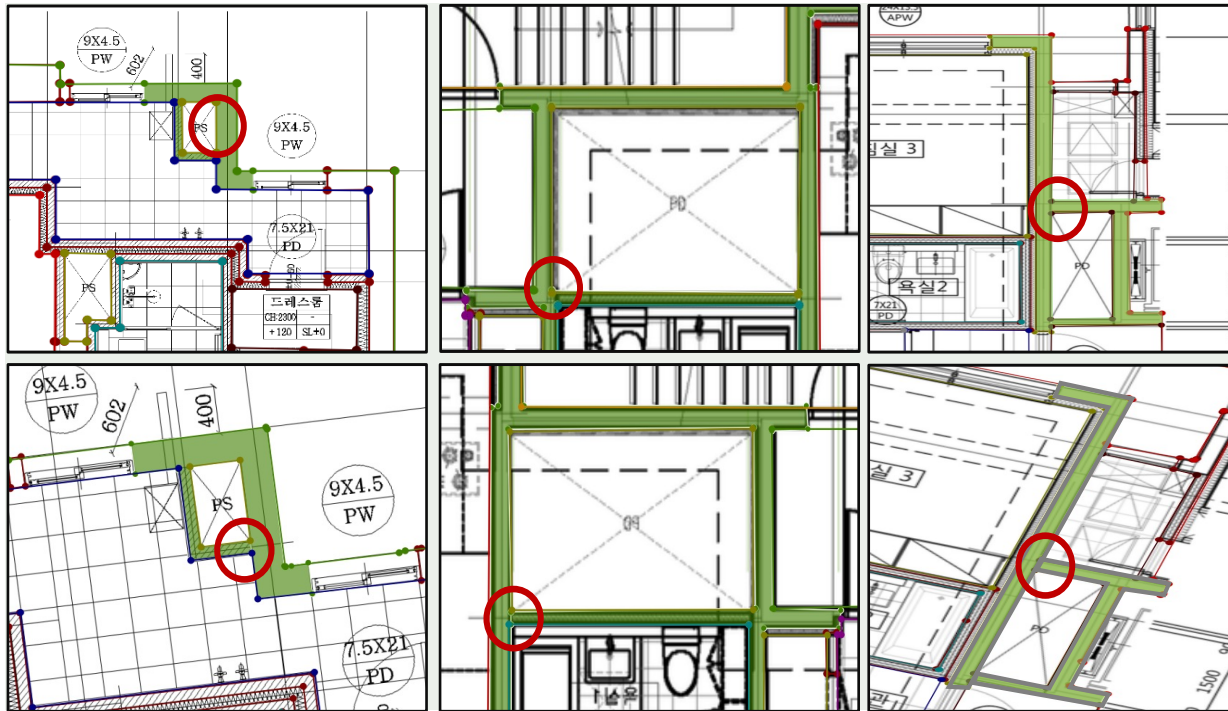


Figure 6. Results produced by the proposed topology-preserving augmentation. The upper row shows the ground truth ring-type polygon annotations, while the lower row presents the augmented outputs generated by our method. The red circles highlight locations where the bridge connections between the outer and inner boundaries are preserved after augmentation, maintaining the cyclic polygon chain and preventing topology fragmentation.

(Figure 6). The resulting polygons therefore maintain a single closed cyclic representation while preserving the correct outer–inner boundary relationships without introducing redundant vertices.

Performance across multiple geometric transformations is summarized in Table 3. Cyclic adjacency preservation remains close to unity for all augmentation types, including compound transformations such as rotation combined with cropping. These results indicate that the proposed repair strategy remains robust under a wide range of geometric transformations commonly used in polygon-based segmentation pipelines.

Overall, the results demonstrate that enforcing successor consistency in index space effectively preserves polygon topology during geometric augmentation and enables reliable integration of augmentation pipelines in polygon-based segmentation workflows.

Effect of Topology Preservation on Segmentation Training: To assess the practical impact of topology preservation, we train segmentation models using datasets augmented with different pipelines and compare standard augmentation with the proposed topology-preserving strategy.

Two segmentation architectures are evaluated: YOLOv11-

Seg and Mask R-CNN. All models are trained with identical hyperparameters and evaluated using mean Intersection over Union (mIoU).

Experiments are conducted on a dataset of approximately 600 Korean floorplan images with polygon-based segmentation annotations for architectural regions. The dataset is divided into training, validation, and test sets using a 70%, 20%, and 10% split.

Geometric augmentation is applied only to the training set to increase data diversity. For each training image, five augmented samples are generated using random transformations sampled from the parameter ranges listed in Table 1. The same augmentation settings are used for both baseline and topology-preserving pipelines to ensure a fair comparison.

Table 4. Segmentation performance using different augmentation strategies.

Method	mIoU \uparrow
YOLOv11-Seg (Std. Aug.)	88.4
YOLOv11-Seg (Ours)	90.8
Mask R-CNN (Std. Aug.)	85.2
Mask R-CNN (Ours)	87.0

The dataset used in this study is publicly available through the AI Hub platform (<https://aihub.or.kr/>).

The results indicate that preserving polygon topology during augmentation improves segmentation performance. Models trained with topology-consistent annotations achieve higher mIoU and produce more accurate boundary predictions, suggesting that eliminating structural inconsistencies in augmented annotations allows the models to learn geometric boundaries more reliably.

6. Code Availability

The implementation is publicly available as a Python package and can be installed via:

```
pip install polyaug
```

The source code and experimental scripts are available at:

<https://github.com/Laudarisd/polyaug>

7. Conclusion

This work studies the structural impact of geometric data augmentation on polygon-based segmentation annotations. Although geometric transformations theoretically preserve polygon geometry, practical augmentation pipelines often remove vertices during clipping or cropping, breaking the cyclic adjacency relations that define ring-type regions.

Using the proposed Cyclic Adjacency Preservation (CAP) metric, our experiments show that common augmentation workflows frequently introduce structural discontinuities in polygon annotations. In contrast, enforcing index-consistent connectivity preserves the cyclic structure of polygons across a wide range of geometric transformations.

These findings highlight the importance of maintaining annotation-level topology during data augmentation. While motivated by ring-type regions commonly found in architectural datasets, the proposed index-aware repair principle can be applied to general polygon annotations where vertex ordering encodes structural relationships. Preserving such structural consistency can improve the reliability of polygon-based segmentation pipelines and downstream geometric learning tasks.

References

Acuna, D., Ling, H., Kar, A., and Fidler, S. Efficient interactive annotation of segmentation datasets with polygon-rnn++. In *Proceedings of the IEEE conference on Computer Vision and Pattern Recognition*, pp. 859–868, 2018.

Benenson, R., Popov, S., and Ferrari, V. Large-scale interactive object segmentation with human annotators. In *Proceedings of the IEEE/CVF conference on computer vision and pattern recognition*, pp. 11700–11709, 2019.

Bloice, M. D., Stocker, C., and Holzinger, A. Augmentor: an image augmentation library for machine learning. *arXiv preprint arXiv:1708.04680*, 2017.

Bochkovskiy, A., Wang, C.-Y., and Liao, H.-Y. M. Yolov4: Optimal speed and accuracy of object detection. *arXiv preprint arXiv:2004.10934*, 2020.

Buslaev, A., Iglovikov, V. I., Khvedchenya, E., Parinov, A., Druzhinin, M., and Kalinin, A. A. Albumentations: Fast and flexible image augmentations. *Information*, 11(2): 125, 2020. doi: 10.3390/info11020125.

Carlsson, G. Topology and data. *Bulletin of the American Mathematical Society*, 46(2):255–308, 2009. doi: 10.1090/S0273-0979-09-01249-X.

Chen, Y., Li, Y., Kong, T., Qi, L., Chu, R., Li, L., and Jia, J. Scale-aware automatic augmentation for object detection. In *Proceedings of the IEEE/CVF conference on computer vision and pattern recognition*, pp. 9563–9572, 2021.

Chen, Y., Zhang, P., Kong, T., Li, Y., Zhang, X., Qi, L., Sun, J., and Jia, J. Scale-aware automatic augmentations for object detection with dynamic training. *IEEE Transactions on Pattern Analysis and Machine Intelligence*, 45(2):2367–2383, 2022.

Cordts, M., Omran, M., Ramos, S., Rehfeld, T., Enzweiler, M., Benenson, R., Franke, U., Roth, S., and Schiele, B. The cityscapes dataset for semantic urban scene understanding. In *Proceedings of the IEEE conference on computer vision and pattern recognition*, pp. 3213–3223, 2016.

Dodge, S., Xu, J., and Stenger, B. Parsing floor plan images. In *2017 Fifteenth IAPR international conference on machine vision applications (MVA)*, pp. 358–361. IEEE, 2017.

Edelsbrunner, H., Harer, J., et al. Persistent homology—a survey. *Contemporary mathematics*, 453(26):257–282, 2008.

Ghahremani, T., Hoseyni, M., Ahmadi, M. J., Mehrabi, P., and Nikoofard, A. Augmentory: A fast and flexible polygon augmentation library. *arXiv preprint arXiv:2405.04442*, 2024.

Girard, N., Smirnov, D., Solomon, J., and Tarabalka, Y. Polygonal building extraction by frame field learning. In *Proceedings of the IEEE/CVF Conference on Computer Vision and Pattern Recognition*, pp. 5891–5900, 2021.

Hu, X., Li, F., Samaras, D., and Chen, C. Topology-preserving deep image segmentation. *Advances in neural information processing systems*, 32, 2019.

- Jung, A. imgaug, 2018. <https://github.com/aleju/imgaug>.
- Kaleva, A. and Kämäräinen, J.-K. Cubicasa5k: A dataset and an improved multi-task model for floorplan image analysis. In *Scandinavian Conference on Image Analysis*, 2019.
- Krizhevsky, A., Sutskever, I., and Hinton, G. E. Imagenet classification with deep convolutional neural networks. *Advances in neural information processing systems*, 25, 2012.
- Lazarow, J., Xu, W., and Tu, Z. Instance segmentation with mask-supervised polygonal regression transformers. In *IEEE Computer Society Conference on Computer Vision and Pattern Recognition*, 2022.
- Liang, J., Homayounfar, N., Ma, W.-C., Xiong, Y., Hu, R., and Urtasun, R. Polytransform: Deep polygon transformer for instance segmentation. In *Proceedings of the IEEE/CVF conference on computer vision and pattern recognition*, pp. 9131–9140, 2020.
- Lin, T.-Y., Maire, M., Belongie, S., Hays, J., Perona, P., Ramanan, D., Dollár, P., and Zitnick, C. L. Microsoft coco: Common objects in context. In *European Conference on Computer Vision (ECCV)*, pp. 740–755, 2014. doi: 10.1007/978-3-319-10602-1_48.
- Liu, C., Wu, J., and Furukawa, Y. Floornet: A unified framework for floorplan reconstruction from 3d scans. In *Proceedings of the European conference on computer vision (ECCV)*, pp. 201–217, 2018.
- Long, J., Shelhamer, E., and Darrell, T. Fully convolutional networks for semantic segmentation. In *Proceedings of the IEEE conference on computer vision and pattern recognition*, pp. 3431–3440, 2015.
- Mikolajczyk, K., Tuytelaars, T., Schmid, C., Zisserman, A., Matas, J., Schaffalitzky, F., Kadir, T., and Gool, L. V. A comparison of affine region detectors: Mikolajczyk et al. *International journal of computer vision*, 65(1):43–72, 2005.
- Mnih, V. *Machine learning for aerial image labeling*. University of Toronto (Canada), 2013.
- Myshkovskiy, Y., Nazarkevych, M., Vysotska, V., and Yurynets, R. Exponential data augmentation methods for improving yolo performance in computer vision tasks. 2025.
- Perez, L. and Wang, J. The effectiveness of data augmentation in image classification using deep learning. *arXiv preprint arXiv:1712.04621*, 2017.
- Roboflow, Inc. Roboflow: Annotation and augmentation platform. <https://roboflow.com>, 2023.
- Ronneberger, O., Fischer, P., and Brox, T. U-net: Convolutional networks for biomedical image segmentation. In *International Conference on Medical image computing and computer-assisted intervention*, pp. 234–241. Springer, 2015.
- Russell, B. C., Torralba, A., Murphy, K. P., and Freeman, W. T. Labelme: a database and web-based tool for image annotation. *International journal of computer vision*, 77(1):157–173, 2008.
- Shorten, C. and Khoshgoftaar, T. M. A survey on image data augmentation for deep learning. *Journal of Big Data*, 6(1):60, 2019. doi: 10.1186/s40537-019-0197-0.
- Ultralytics. Yolov11: Real-time object detection. <https://github.com/ultralytics/ultralytics>, 2024.
- Zheng, J., Li, Y., et al. Structured3d: A large photo-realistic dataset for structured 3d modeling. In *ECCV*, 2020.
- Zoph, B., Cubuk, E. D., Ghiasi, G., Lin, T.-Y., Shlens, J., and Le, Q. V. Learning data augmentation strategies for object detection. In *European conference on computer vision*, pp. 566–583. Springer, 2020.